IDŐJÁRÁS

Quarterly Journal of the Hungarian Meteorological Service
Vol. 121, No. 3, July – September, 2017, pp. 209–241

Satellite retrieval of severe storms based on the cloud microphysical profile over Central Europe

Michal Pokorny* and **Michal Zak**

Faculty of Mathematics and Physics, Charles University, V Holesovickach 2, Prague 8, 180 00, Czech Republic

**Corresponding author E-mail: mich.pok@seznam.cz*

(Manuscript received in final form August 31, 2016)

Abstract—The analysis of profiles of temperature (*T*) with regard to the effective radius (*re*) of cloud particles shows the vertical distribution of the effective particle size in clouds. The profiles are computed and constructed from satellite retrieved data and show graphically the distribution of the cloud particle size focused on convective clouds and convective storms subsequently. This special technique of severe storm analysis and forecasting, developed by *Rosenfeld et al.* (1998), has been tested in several countries around the world. Forecasting and predicting dangerous phenomena such as hailstorms or tornadoes that occur in severe storms is the main objective of this technique. This nowcasting tool is now also being tested in Central Europe for the first time. The basic description of the theory is presented in this paper including the results of our research, which confirms application of the theory in Central Europe in severe storm nowcasting. One typical severe and one nonsevere storm event in the Czech Republic and their vicinity are selected and described to show the main difference of *T-re* profiles in distinguishing of severe weather forecast. Furthermore, this paper discusses the possible benefits of this method for the Czech Weather Service, because it clearly reveals severe storm development in the monitored area.

Key-words: *T-re* profiles, severe storm, cloud particles, satellite observation, storm nowcasting

1. Introduction

Severe convective storms occur over Central Europe mostly in the warm season, and in some regions their reports become more frequent every year (*Holzer*, 2001; *Horváth* and *Geresdi*, 2003; *Tolasz et al.*, 2007; *Dotzek et al.*, 2009). The accompanying phenomena of convective storms represent a big hazard, and it is evident that Europeans are affected by severe convective weather hazards as well (*Doswel*, 2014).

Every year, tornadoes are detected in Central Europe (*Dotzek*, 2003). There is a clear increase in tornado frequency from the past to present (*Brázdil et al.*, 2012). The highest frequency of tornado reports in the Czech Republic is in the summer half of the year (June-August): 65.7%. Tornado may cause serious regional or local damage or even number of casualties. These events connected to convective storms have also hit densely populated regions in the past few years, and thus increased their threat (*Doswel*, 2014).

It is very important to consider the possible impacts on severe weather events such as thunderstorms and tornadoes as the climate on Earth changes (e.g., *Brooks*, 2012). A CAPE increase is expected in the future from climate model simulations, which will lead to more frequent environments favorable for severe storm occurrence (*Brooks*, 2012). Local increases in heavy rain (*Field et al.*, 2012) and severe tornadoes (*Doswel*, 2014) are expected in the future, larger hail reaching the ground may also be expected (*Brooks*, 2012).

It is essential to be able to forecast the possible occurrence and impact of severe weather events. Severe storms must be identified as early as possible to the timely warning issued before the storm hits populated areas. Nowcasting tools play a major role in this matter. Different nowcasting and forecasting methods based on satellite and radar data are used in different countries and a lot of them are under further development. The main feature (and also the main "problem" for the forecasting) of convective storms, however, is their rapid development, small scale, and short life. These features were not so easy to track (*Shiqiang* and *Zhemin*, 2001) using the first generation geostationary satellites 15 years ago. Now, that modern geostationary satellites and radar observations are used, tracking is much easier. Recent multi-spectral satellite capabilities in meteorology (GOES and MSG) can be used to identify the start of glaciation in elevating cloud tops, to augment the techniques by *Roberts* and *Rutledge* (2003). In addition, the sounding capabilities of both satellites can be used to monitor changes in precipitable water and thermodynamic stability (CAPE and CIN) in cloud-free areas prior to storm initiation, and within the near-surface inflow to existing storms (http://www.ssec.wisc.edu/~rabin/paper/eumetsat/paper2_eumetsat.doc).

Current storm nowcasting in the Czech Republic is mostly based on radar and satellite data (both are available every five minutes). Available weather radar data used in Central Europe, e.g., http://radar.bourky.cz/ (2015), reveal only precipitating clouds as they occur. Such data are not able to analyze the pre-storm environment and cannot provide any specific information as to what dangerous phenomena can occur (if large or small hail or tornadoes). Weather model output refers to a specific time of input data and do not respond to the ongoing atmospheric processes. For nowcasting, they provide only little information. Thus, it is very useful to supplement it with a tool which is able to analyze the above mentioned pre-storm environment and to provide any specification in the field of developing storms before the current systems are able to identify them. Such a tool would provide more time for a forecaster to issue any relevant warning or specific forecast of severe and hazardous weather.

These microphysical characteristics of the pre-storm environment of clouds can now be gained by analyzing the profiles of temperature and the size of cloud particles as introduced by *Rosenfeld* and *Lensky* (1998). These profiles express the effective cloud particle radius (*re*) and temperature (*T*) (*Rosenfeld* and *Lensky*, 1998; *Rosenfeld et al*., 2008), and they indirectly reveal the updraft strength.

A nowcasting tool based on *T-re* profiles has been tested for the Central European region for the first time, and it is expected to improve forecasters' skills. On the basis of good results in several testing processes, it is expected to be confirmed as a new simple auxiliary forecasting tool in the region of Central Europe as well as in the field of dangerous weather event forecasting and other meteorological applications. Its simplicity lies in the use of Meteosat geostationary data in the frame of MSG_RGB software provided by its developer *I. M. Lensky* which was developed especially for the view of *T-re* profiles. The documentation of the software was provided by its developer Lensky in 2009. The main aim of this study is to improve accuracy of severe storm nowcasting so that damage and serious injuries are prevented and life protection is strengthened in Central Europe.

Section 2 describes the origin and basic principles of the applied method, Section 3 mentions the procedure of processing the data. The following part then introduces the profiles of severe and nonsevere situations and conveys more profound analysis of typical severe and nonsevere situations. Setion 4 compares the collected data from both situation types.

2. Method

Rosenfeld and *Lensky* introduced the technique of *T-re* profiles (*T* - particle temperature, *re* - particle effective radius) in forecasting severe storms and their accompanying dangerous phenomena such as hail and tornadoes (*Rosenfeld* and *Lensky*, 2008). This technique was used in different projects (*Rosenfeld et al*., 2006; *Rosenfeld et al*., 2008), and tests were carried out and verified (*Lensky* and *Rosenfeld*, 2006) in several countries (namely Israel, California, Texas, Brazil, and in Africa) with different satellites providing 3.9 or 3.7 μm spectral information. MSG (Meteosat Second Generation) geostationary satellite data were previously used in *T-re* profiles testing in the Mediterranean Sea area (*Lensky* and *Shiff*, 2007). In addition, other applications of the MSG data in the conditions of Central Europe were applied (*Pfeifer et al*., 2010). MSG data enable to track the evolution of the effective radius of cloud particles with the cloud top temperature by the *T-re* method also in Central Europe. The geostationary satellite MSG provides data scanned from a stable position, which is more useful for the continuous tracking of images compared to polar orbiting satellites. It was decided not to test the data from the polar orbiting satellite due to their irregular time resolution in our territory. There is no need to recalculate MSG data for any other satellite position, which is another big advantage compared to polar orbiting satellites. Another benefit is the frequency of cloud scanning, which is five minutes in the rapid scan mode. MSG has some other advantages for cloud observation such as 12 spectral channels or a higher resolution of images (as good as 1 km). In the region of Central Europe the resolution is lower, approximately 3 km, which is a lower resolution compared to polar orbiting satellites. With the new generation of Meteosat satellites, the resolution will be higher. To analyze the cloud top temperature and the effective radius of cloud particles in this work, the MSG geostationary satellite data and generated *T-re* profiles are applied for the area of Central Europe. The most advantageous procedure is to start the analysis with first convective clouds and track their evolution in consecutive MSG images before they become severe.

2.1. T-re profile principles

The method of *T-re* (*Rosenfeld et al*., 2008) profiles was designed to reveal the microphysical characteristic (*Rosenfeld et al.,* 2008) of severe storm clouds influenced by updraft speed (*Rosenfeld et al.,* 2008). Microphysical vertical profile as a function of temperature or height inside clouds may be explained as follows. Initially, cloud droplets at the bottom of a cloud grow by water vapor diffusion processes, followed by the second zone of collision-coalescence situated above. In the third stage, the droplets have already reached sizes large enough to enable internal precipitation processes. The fourth zone is mixed phase where ice and water coexist and further enhance the growth of droplet efficiency and the droplets grow even faster. The upper glaciated stage, where all the droplets are frozen, is situated above the level of –38 °C (*Rosenfeld et al*., 2008). Each zone has a different slope of the percentile line in *T-re* diagrams, which enables their identification (*Martins et al.*, 2007). A more profound interpretation of microphysical layers in clouds and the above mentioned features is provided by *Lensky* and *Rosenfeld* (2005).

We will focus on the *T-re* profile as a graphical tool to reveal the severity of a developing storm (either in one type of airmass or in the vicinity of frontal boundaries) before it reaches the severe stage. Selecting a group of cells intentionally at different stages of development for the creation of *T-re* profiles indirectly helps to determine the updraft strength inside clouds and to estimate the storm severity subsequently. The vertical updraft speed in clouds is the main factor in distinguishing between stratiform and convective cloud types. In stratiform clouds, the ascending air speed is low, so the cloud particles usually grow to larger sizes at lower levels compared to the situation in deep convective clouds. Conversely, in convective clouds, particles have to overcome the above mentioned updraft strength to fall out of the cloud to become precipitation (*Tokay* and *Short*, 1996). In addition, severe convective storms always produce hazardous weather events, such as tornadoes, hail, damaging wind, and so forth (*Jurkovic et al*., 2015). Such events occur in convective systems entirely due to the updraft motion (*Jurkovic et al*., 2015). Cloud particle size is related to the updraft strength inside convective clouds or storms which are developing within the target area. Thus, the particle size indirectly represents the severity of developing storms. The role of the updraft strength in the formation of severe weather can be explained as follows. The higher speed of the updraft delays the growth of cloud particles to larger sizes and postpones their glaciation. In other words, when there is a strong updraft in a cloud, particles do not have enough time to grow to larger sizes because they ascend through the cloud very quickly upwards. *T-re* profiles obtained and computed from satellite data by the MSG_RGB software indirectly reflect the updraft speed in rapidly growing convective clouds. In the case of vigorous convection, these profiles usually show only small particles near the cloud tops of relevant cumulonimbus clouds compared to nonsevere cases. Typical profiles of severe and nonsevere storms in maritime and continental conditions are provided by *Rosenfeld et al*. (2008).

The MSG_RGB software provides multispectral information on MSG channels for generating *T-re* profiles. The 3.9 μm reflectance determinates the cloud particles size in generated profiles. Smaller cloud particles are revealed by a larger 3.9 μm reflectance. According to some studies, it has been shown that smaller crystals are really effective reflectors near 3.9 μm (e.g., *Melani et al*., 2003). The major hypothesis assumes that such detection of cloud cells with the enhanced 3.9 μm reflectivity due to small cloud particles discloses rapidly developing thunderstorms with a high updraft speed inside clouds.

The *T-re* analysis tool performs all calculations automatically as it was developed to generate *T-re* profiles in a graphical form without any additional calculations. Its main goal is to provide such graphical output that enables quick reaction to the severity of a developing storm. Unfortunately, the software cannot reduce the number of lines in profiles. Nevertheless, the *T-re* method was designed to be as easy and fast as possible.

Because of the 3.9 μm channel features (*Setvák*, 1989), the method is limited to daytime hours only, when solar illumination is available. This limitation is also mentioned by *Jurkovic et al*. (2015). This aspect poses the major deficiency of this tool, because many convective storms keep developing after sunset. After personal communication with Prof. *D. Rosenfeld* in 2015 concerning the issues of

T-re profile method, the limit for solar zenith angle was set to be 65°. In addition, there is no possibility to show country borders in the background of an image for better orientation in the satellite image, which is another disadvantage of the *T-re* method in MSG_RGB software.

In addition, in a recently published study (*Sporre et al*., 2014) from another European region, *T-re* profiles were also used to find cloud particle sizes. This paper focuses on analyzing aerosol effects on convective clouds. However, the detected cloud drop size range corresponded to our data. *Zipori et al*. (2015) have recently used the same technique with the MSG_RGB program (*Lensky* and *Rosenfeld*, 2008) and the satellite data of Meteosat-9 in their study of the effect of aerosol sources on cloud particle size and glaciation temperature. *Jurkovic et al*. (2015) used the MSG 3.9 μm reflectivity for generating the profiles of cloud effective radius and temperature (*T-re*) to describe severe storms characteristics over Central Europe. They applied *Rosenfeld* and *Lensky's* (1998) methodology in Hungary, Germany, Austria, and other countries. *Rosenfeld et al*. (2013) employed the theory of *T-re* profiles (*Rosenfeld* and *Lensky*, 2008) in the study of cloud microstructure. The vertical evolution of cloud microstructure using the above mentioned methodology was also used in warm rain onset height and aerosol optical depth research (*Zhu et al*. 2015). They mentioned some basic rules concerning *T-re* profiles, which are also used in our paper. *Zheng* and *Rosenfeld* (2015) studied the updraft speed in convective clouds according to *Rosenfeld et al*. (2014) and *Zheng et al*. (2015) in another project.

3. Data from T-re profiles

The principles described above were tested on data from the warm part (from May to August) of the years 2005–2013 for the Czech Republic and its vicinity on archive data provided by EUMETSAT. Subsequently, another test was realized on real-time data of the years 2012–2013 for days, when intensive accompanying phenomena of convective storms were expected (forecasted) or reported (for archive data). These data were selected according to the severity of storms; the severity criteria were mainly based on the European Severe Weather Database (ESWD) (http://www.eswd.eu/) operated by the ESSL (European Severe Storms Laboratory). In general, ESWD provides a clear description of severe weather events online (http://www.eswd.eu/cgi-bin/eswd.cgi?action=showdefinitions &lang=en_0) and the list of severe weather event reports online. Similarly, *Jurkovic et al*. (2015) define the warm part of the year as May-September.

52 situations with strong convection or rain occurrence were analyzed. While 33 of those were accompanied by severe attendant phenomena, 17 situations may be classified as nonsevere. From all severe situations, 24 hit the Czech Republic. Subsequently, after detailed analysis of the selected severe and nonsevere situations, a table of tracked values of the *T-re* profiles was compiled (*Table 1*)

and is provided in Section 5. The values of tracked features mentioned below can be simply gained from the numerical listing of temperatures (in 1 °C steps) and the radii related for each percentile line depicted in the *T-re* profile. This is very useful for further computations. Graphically the values could be acquired from the generated *T-re* profiles, which is possible due to the good resolution of the *T-re* profiles. As a matter of fact, *Tl* or *Tg* are the breaking points of the 15th percentile line in the profile, i.e., the vertical coordinate of the 15th percentile line, which makes them easy to recognize in the gained *T-re* profiles. This can mostly be used to make a quick reaction to the severity of a storm.

An analysis of the severe situation data is shown in *Figs. 1a-f* based on satellite data obtained from the EUMETSAT archive and the MSG reception station (situated in the Dept. of Atmospheric Physic, the Faculty of Mathematics and Physics, Charles University, Prague) and processed in the MSG_RGB software (*Lensky*, 2009). An analysis of the nonsevere situation data is shown in *Fig. 2*, which is based on the Severe Storm product. Section Four provides information about collecting the data, *Table 1* in Section Five summarizes the typical features of *re*, *Tl*, *Tg,* and so forth, of selected situations, and *Table 2* provides their statistical processing.

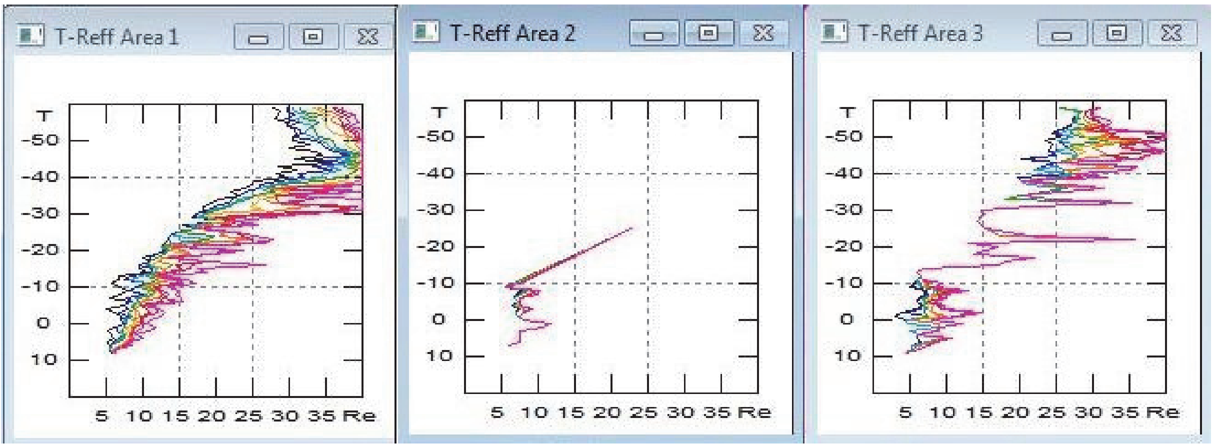

Fig. 1a. Analysis of the situation for 1457 UTC, June 12, 2010

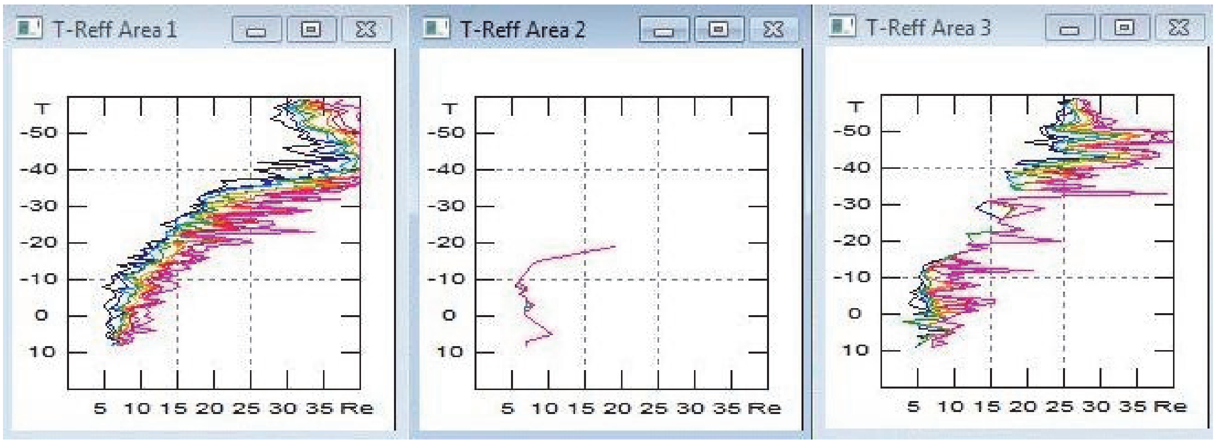

Fig. 1b. The same as *Fig. 1a* but for 1512 UTC, June 12, 2010

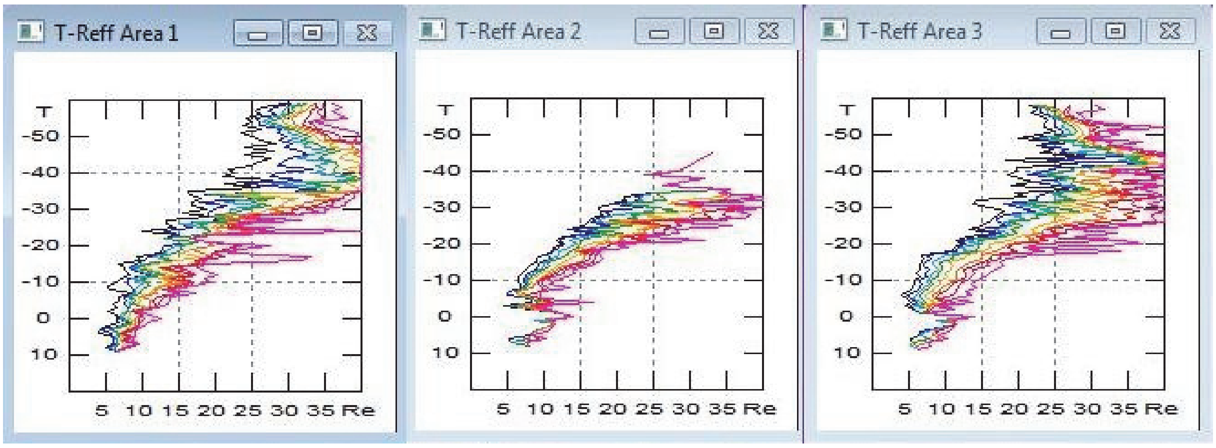

Fig. 1c. The same as *Fig. 1a* but for 1542 UTC, June 12, 2010

Re (μm) – cloud particle radius
T (°C) – temperature of cloud particle
Color lines (black to magenta) in profiles express the 5th to 100th percentiles of effective particle radius in the interval of 1 °C.

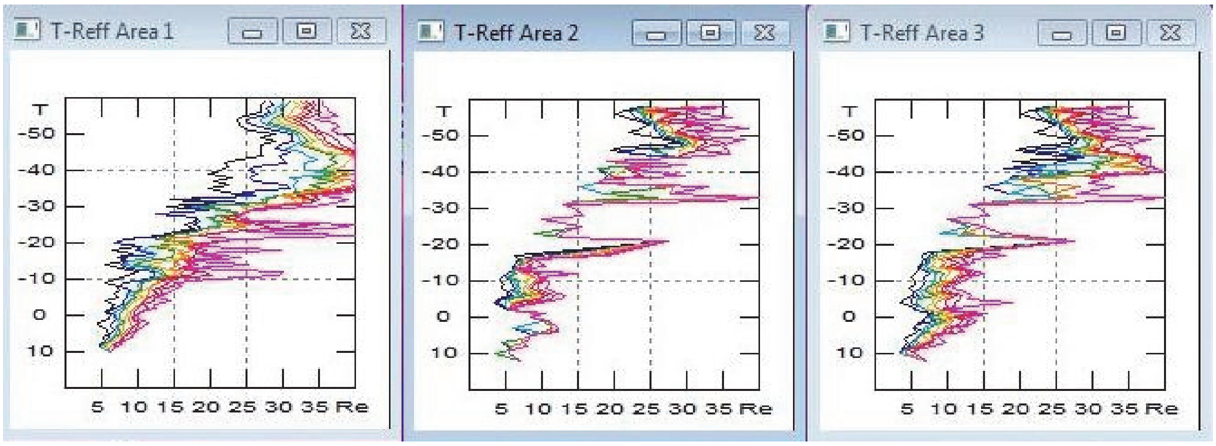

Fig. 1d. The same as *Fig. 1a* but for 1557 UTC, June 12, 2010

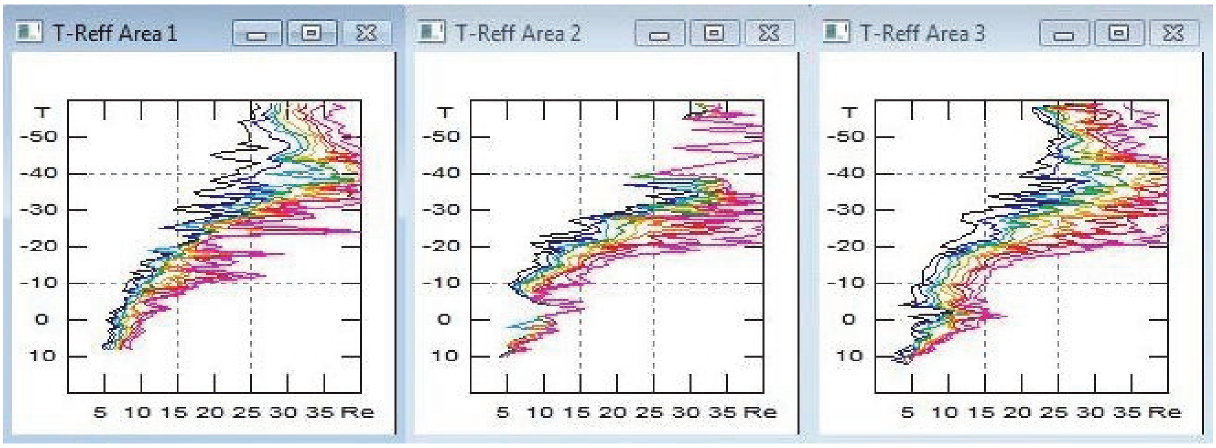

Fig. 1e. The same as *Fig. 1a* but for 1612 UTC. June 12, 2010

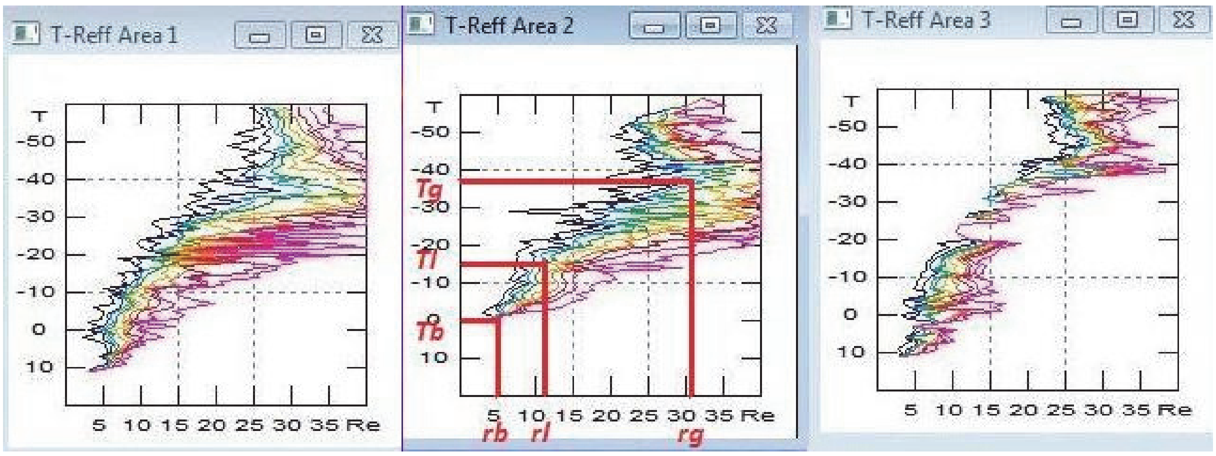

Fig. 1f. The same as *Fig. 1a* but for 1627 UTC. June 12, 2010

Re (µm) – cloud particle radius ; T (°C) – temperature of cloud particle
rb (µm) – cloud particle radius range near the cloud base
rl (µm) – cloud particle radius near the top of the lower linear part of the profile
rg (µm) – temperature of the glaciation phase bottom
Tb (°C) – cloud particle temperature near the cloud base
Tl (°C) – temperature of the top of the lower linear part of the profile, it mostly represents the top of the layer in which the particles grow mostly by diffusional or coalescence growth
Tg (°C) – temperature of the glaciation phase bottom, from this layer, all particles are expected to be frozen, it is the top of the mixed phase layer
Color lines (black to magenta) in profiles express the 5th to 100th percentiles of effective particle radius in the interval of 1 °C.

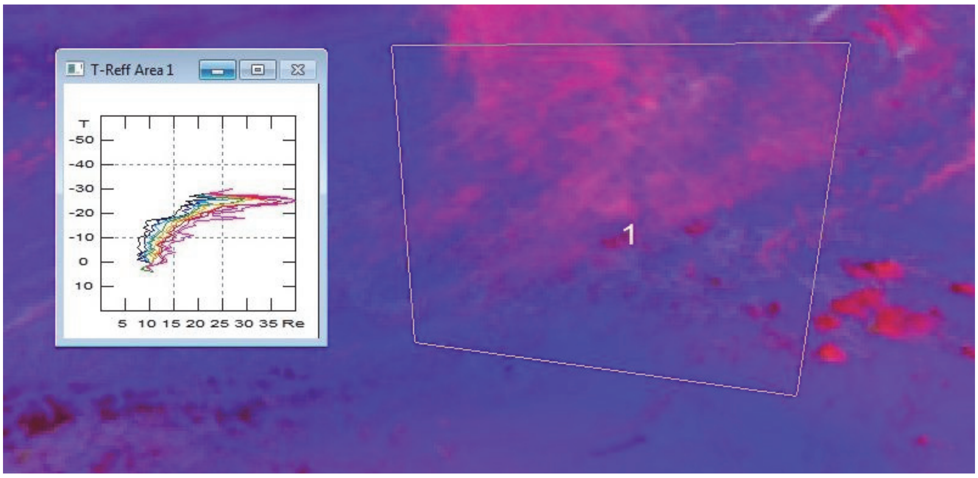

Fig. 2. Analysis of the situation for 1400 UTC. May 23, 2013 – nonsevere profile. Color lines (black to magenta) in profiles are expressing 5th to 100th percentiles of effective particle radius in the interval of 1 °C.

4. T-re profiles in the territory of Central Europe

As already mentioned above, two groups of convective situations (severe and nonsevere) were studied. The areas of convective clouds either moving to Central Europe or developing there were determined, and the satellite images generated from the MSG data were compared. These images were analyzed in a time interval when the solar zenith angle of the Sun was greater than 65°. Within that time period, the reflected sunlight in the 3.9 μm channel was sufficient. In these areas and times, the *T-re* analysis was done, and the data from the saved images were subsequently processed. Afterwards, a forecast of the severity of a storm based on the *T-re* profile shapes and gained values was given immediately as the profiles revealed severe features. Later, it was compared to weather reports and radar observations. A case study was selected from each group to be analyzed in a greater detail for the Central European region. Dangerous phenomena in the severe case and the typical *T-re* features are described.

4.1. Comparison of severe and nonsevere situations

This Chapter introduces the *T-re* profiles of one severe and one nonsevere situation to show their mutual differences. However, it is clear that the temperatures and particle sizes do not match exactly the values which were received from the profiles in other countries (*Rosenfeld et al.*, 2008), because Central European conditions are partly different. For example, cloud base temperatures are usually lower in Central Europe in the warm season, and cloud particles near the cloud base are slightly larger compared to profiles derived, for example, from the USA. For this reason we decided to test this method in the European environment, and we tried to get specific *T-re* shapes for this region.

The shape and position of percentile lines in profiles are the main features of profiles, which can help us to decide if the storm is prone to grow to a severe or nonsevere storm.

In this case, a nonsevere situation means that thunderstorms developed without dangerous accompanied phenomena are classified according to ESWD. The situation represents the threshold state for nonsevere/severe situations. Other weaker or less intensive storms revealed even shallower *T-re* profiles with larger particles at lower levels and cloud tops which did not reach significantly higher levels, i.e., over 6 km, are typically nonsevere profiles.

4.1.1. Case study of June 12, 2010: the severe situation

This situation was chosen as a case study due to the occurrence of a supercell with large hail, heavy rain, and strong wind. It is a typical severe storm with dangerous attendant phenomena. Furthermore, *Figs. 1.a-f* clearly show gradual evolution of *T-re* profiles in Central Europe from 1457 UTC to 1627 UTC after they became severe. Cloud particles grow very slowly to larger sizes, when coalescence and mixing of liquid water with ice particles continues.

A low pressure area moving to the southeast was affecting Central Europe, the temperature maxima in the Czech Republic were about 26 °C. After 1500 UTC, massive Cbs were observed, and thunderstorms developed in the Czech Republic. In southern Bohemia, a supercell formed where a rotation of the cloud system was observed from the ground by witnesses, and a funnel cloud was reported. After 1700 UTC, hail and heavy rain occurred. The hail diameter was about 3 cm. Severe wind gusts were reported after 1800 UTC, followed by heavy precipitation in south of Moravia. After 2000 UTC, other wind gusts were reported in southern Moravia. Strong wind was observed after 1800 UTC in Austria and it was followed by a heavy rain. The wind speed in the squall line was 25 m/s (ESWD).

The analysis of cloud areas in *Fig. 1a* shows very small particles (less than 15 µm in radius) up to about –20 °C in clouds according to *T-re* profiles. This indicates a strong updraft in the lower part of these clouds, namely in area 1 showing a long and nearly linear lower part of the profile which indicates the possibility of a severe weather occurrence (*Rosenfeld et al.*, 2008). This is confirmed by a hail report from South Bohemia and other dangerous phenomena in the vicinity (ESWD). The profiles in *Figs. 1a-1f* are similar to the profiles gained by *Rosenfeld et al*. (2008), when hail and other severe weather events were documented. As early as 1457 UTC, cloudiness with a strong updraft above Austria (*Fig. 1a* – area 1) is revealed by the *T-re* analysis. The profile starts at 9 °C and 6 µm. This indicates the cloud base temperature (*Tb*) to be 9 °C and the effective radius of cloud base particles (*rb*) to be 6 µm, which is in agreement with *Rosenfeld et al*., (2008) and other authors (*Rosenfeld* and *Lensky*, 1998). The top of the zone of coalescence (*Tl* - temperature of the lower linear part of the profile, it mostly represents the top of the layer in which the particles grow mostly by the diffusional or coalescence processes) only reaches –8 °C with a cloud particles' radius at that level (*rl* - cloud particle radius near the top of the lower linear part of the profile) of 8 μm, but the mixed phase zone steeply reaches the *Tg* (temperature of the glaciation zone bottom) of –28 °C and *rg* (radius at *Tg* - temperature of the glaciation phase bottom) of 18 μm. This level indicates the full development of the ice phase inside the cloud and the top of a deep mixed phase. In such clouds, the precipitation is mostly formed by snow particles and hail. Later, the updraft becomes even stronger and fills a vertically higher area. Its extent is from 9 °C (*Tb*) at the cloud base to the level of –16 °C (*Tl*). The particle radius at the cloud base (*rb*) is 6 μm and *rl* (particle radius at *Tl*) is 8 μm. The particles rise in updraft so quickly that they do not have enough time to grow to larger sizes before reaching that level. The top of the mixed phase zone reaches the level of *Tg* of –40 °C with *rg* of 34 μm. The difference between *Tl* and *Tg* is equal to 24 °C, which is quite large. For a high severity storm, the difference is supposed to be as small as possible. Later, the coalescence zone reaches higher levels, and the difference between *Tl* and *Tg* decreases to only 7 °C. This indicates that the severity of the developing storm rises. After 1500 UTC, larger particles in *T-re* profiles appear, and the slope of profiles is not as steep as in the case described above. The regeneration of updrafts (and *T-re* profiles severity) to the previously mentioned values occurs at about 1600 UTC (*Fig. 1f* – area 1) but after 1700 UTC, the clouds are filled with larger particles, and the updrafts weaken again.

Area 2 in *Fig. 1f* (east of Germany, west of the Czech Republic) shows a coalescence zone from 0 °C and an *rb* of 7 μm to –20 °C and 13 μm. The mixed phase continues up to the level of –33 °C with an *rg* of 38 μm. The vertical extent of the small particle zone is shallow, and particles grow fast to larger sizes. This profile thus provides information about a weaker updraft and, according to some of the following images from later hours, it did not reach larger intensity. No severe weather events were reported from that area.

The cloud base temperature (*Fig. 1e* – area 3) was 12 °C and *rb* 3 μm at 1612 UTC. The coalescence zone reaches the level of –26 °C with *rl* 17 μm. The top of the mixed phase zone is then detected at –38 °C level with *rg* 29 μm. Such a profile corresponds to a strong updraft. Later, at about 1700 UTC, that strong updraft rises to the level of –40 °C with *rg* of 15 μm. At least large hail may be predicted with the help of this cloud profile. Particles of such a small radius at this height reveal a significantly severe updraft inside clouds.

4.1.2. Case study of 23May 2013: the nonsevere situation

There are no severe weather reports in ESWD for the May 23rd, 2013. There were thunderstorms observed in the northeast of the Czech Republic according to professional weather station reports. The weather was influenced by the low pressure area.

Since the morning hours, stronger updrafts in the lower part of clouds have been revealed by *T-re* profiles. Cloud base temperature is about 3 °C, and the radius of particles is 6 µm. The coalescence zone reaches the level of –27 °C with *re*12 µm. Later the radius grows to 22 µm. The cloud base temperature changes to -8 °C, and the particle radius changes to 7 µm. A radius of 15 µm is reached at the level of –20 °C. The profiles have nearly linear shape in some parts, but they are bent down to larger particles (to the right side of the profile). *Fig. 2* shows the cloud base temperature at about 4 °C, and the radius of particles at 9 µm. The cloud top reaches –29 °C with particle radius 23 µm. The lower linear part of the profile (coalescence zone) reaches the level of –16 °C with particle radius 14 µm. The cloud tops do not reach any significant height. A fully glaciated zone with small particles typical of severe situations is not developed. The profiles confirm only a nonsevere convection in the observed region.

5. Results

The data for the analysis are stated in *Tables 1* and *2*, and their description follows in the text. *Table 1* is sorted by the following accompanying events of storms, providing the data of analyzed situations:

TOR – tornado (1)
GR – hail (2)
+RA – heavy rain (3)
FC –funnel cloud (4)
NONSEVERE (5)

Consider tornado being the most intensive (dangerous) accompanying event of a storm expressing its intensity, number 1 was assigned as the most intensive case decreasing to number 4 (see *Figs. 3* and *5*). The intensity decreases from tornado (1) through hail (2) and heavy rain (3) to funnel cloud (4) as mentioned above with respect to the danger for human and infrastructure. The nonsevere category is represented by the number (5).

The description (intensity) of each event (size of hail, length of funnel cloud and so forth) is mentioned in *Table 1* if it was provided by sources (ESWD). Additional information about the date and place of the event is stated together with the time of the forecast of the severe event. This forecast was made according to the analyzed profiles. The analyzed features of the *T-re* profiles in *Table 1* are provided as follows: *re* (µm), *re base* (µm), *re top* (µm), *Tl* (°C), *Tg* (°C), *T14 µm* (°C).

Table 1. Reported severe weather events, nonsevere situations and analyzed values of *re*, *Tl*, *Tg* and *T14μm*

Date	Month	Country	Event	Other event	Attendant phenomena	Time of report (UTC)	Forecast of dangerous event (UTC)	*re* (μm)	*re base* (μm)	*re top* (μm)	*Tl* (°C)	*Tg* (°C)	*T14μm* (°C)
May 23, 2005	5	PL	TOR	GR		1800	1300	6-38	6	38	-28	-38	-28
May 16, 2006	5	FR	TOR	GR	hail 3 cm	1337	1212	4-38	4	38	-15	-33	-15
May 26, 2007	5	D	TOR	GR	F1T3 - 11 km x 200 m path, hail 3 cm	1550	1212	6-33	6	33	-35	-48	-35
Jun 25, 2006	6	D	TOR	GR	F1T3 - 3 km x 300 m path, hail 3 cm	1630	1242	7-28	7	28	-28	-42	-28
Jun 21, 2011	6	CZE	TOR		F1T3 - 9km path	1509	1342 (GR)	9-40	7	40	-20	-38	-15
Jul 23, 2010	7	FR	TOR		0,5 km x 30 m path, hail 5 cm	1600	1112	7-40	7	40	-25	-30	-30
Jul 23, 2010	7	IT	TOR	GR	hail 7 cm	1630	1042	6-40	6	40	-20	-30	-25
Jul 29, 2013	7	CZE	TOR	RA	F1T3, rain 50 mm/h	after 2000	1157	6-36	6	36	-30	-40	-20
Apr 20, 2012	4	CZE	GR		hail 2 cm	1230	1230	6-33	6	33	-22	-30	-22
May 22, 2010	5	CZE	GR		hail 0.5 cm	1100-1500	0757	8-40	8	40	-12	-32	-17
May 27, 2010	5	CZE	GR	FC	hail 3,5 cm, 50 % cloud to ground	1730	1342	7-40	7	40	-24	-31	-27
May 10, 2011	5	D	GR	+RA		1935	1457	5-29	5	29	-32	-40	-28
May 20, 2011	5	D	GR	+RA	rain 60 mm/h, hail 2 cm	1400-1700	1227	7-38	7	38	-27	-35	-20
May 20, 2011	5	PL	GR	+RA	hail 2,5 cm	1400-1800	1227	7-38	7	38	-27	-35	-20
May 2, 2012	5	D	GR		hail 2,5 cm	1800	1142	5-32	5	32	-30	-38	-22
May 3, 2012	5	PL	GR		hail 2-3 cm	after 1100	0845	6-28	6	28	-28	-40	-28
May 4, 2012	5	PL	GR	FC	hail 2 cm	after 1400	0715	6-38	6	38	-20	-32	-25
May 7, 2013	5	PL	GR	FC	hail 3,5 cm, 50 % cloud to ground	after 1400	0715	7-32	7	32	-25	-38	-29
May 8, 2013	5	CZE	GR	FC	hail 3 cm, rain 33 mm/h	1350	1100	4-32	5	32	-36	-38	-28
May 9, 2013	5	PL	GR		hail 3 cm	after 1500	0630	7-20	7	20	-15	-38	-20
Jun 12, 2010	6	PL	GR		hail 3-10 cm	1840	1427	6-35	6	35	-29	-35	-29
Jun 30, 2010	6	CZE	GR		hail 0,2-1 cm	1330	1142	4-30	5	30	-25	-31	-27
Jun 30, 2010	6	D	GR		hail 3 cm	1500	1257	6-33	6	33	-15	-41	-25
Jun 30, 2010	6	SVK	GR		hail 2 cm		1257	5-33	5	33	-12	-36	-17

Table 1. (continued)

Date	Month	Country	Event	Other event	Attendant phenomena	Time of report (UTC)	Forecast of dangerous event (UTC)	*re* (μm)	*re base* (μm)	*re top* (μm)	*Tl* (°C)	*Tg* (°C)	*T14μm* (°C)
Jul 19, 2007	7	D	GR	+RA	hail 3 cm	1500	0804	7-32	7	32	-20	-38	-27
Jul 19, 2007	7	CZE	GR			1800	1339	7-33	7	33	-25	-38	-27
Jul 19, 2007	7	PL	GR			2000	1204	7-33	7	33	-25	-38	-27
Jul 1, 2009	7	D	GR	FC	hail 4 cm, 40 % cloud to ground	1627	1242	11-38	11	38	-12	-24	-12
Aug 15, 2010	8	CZE	GR		hail 3-5 cm	1900	0927	6-35	6	35	-18	-38	-20
May 31, 2011	5	CZE+A+D	+RA			after 2000	1442	6-33	7	33	-20	-33	-22
Jun 24, 2013	6	PL	FC		35% cloud to ground	1630	0830	7-35	7	35	-25	-35	-25
Jul 19, 2013	7	A	FC		30% cloud to ground	1400-1600	1354	7-12	7	35	-12	-30	-15
Aug 9, 2011	8	CZE	FC		35 % cloud to ground	after 1900		8-40	8	40	-22		-22
Nonsevere situations													
Apr 23, 2013	4	CZE						8-30	8	30	-20	-30	-25
May 12, 2013	5	CZE						9-40	9	40	-22		-24
Jun 7, 2013	6	CZE						10-40	10	40	-18	-31	-18
Jul 20, 2013	7	CZE						8-18	8	28	-10		-12

CZE - Czech Republic
A - Austria
PL - Poland
D - Germany

SVK - Slovak Republic
FR - France
IT - Italy

TOR - tornado
GR - hail
+RA - heavy rain
FC - funel cloud

The values of *rb* (cloud particle radius near the cloud base), *rl* (cloud particle radius near the top of the lower linear part of the profile), *rg* (temperature of the glaciation phase bottom), *Tb* (cloud particle temperature near the cloud base), *Tl* (temperature of the top of the lower linear part of the profile), and *Tg* (temperature of the glaciation phase bottom) are graphically shown in *Fig. 1f* to be understood better. From here, these temperatures and radii abbreviations are used in the text for faster and better orientation.

The cloud base particle radius provides information about the starting point of the evolution of clouds. The smaller the cloud base particle radius is, the more severe event can be expected (*Rosenfeld et al.*, 2008), considering other cloud features such as *Tl*, *Tg,* etc., as confirmed in *Table 2*. For example, in situations with tornado occurrence, the cloud base particle radius was 6.1±0.9 μm, 7.0±0.0, with heavy rain, and 8.8±0.8 μm in nonsevere cases.

On the other hand, the particle radius at the cloud top provides information about the size of particles in the highest part of the cloud. It helps to uncover the intensity of updrafts reaching the cloud top. Smaller particles near the cloud top indicate stronger updrafts pervading through the whole cloud cell. Large particles near the cloud top indicate a weakening updraft at higher levels.

The temperature at the top of the lower linear part of the profile and the temperature of the glaciation phase bottom provide information about the severity of a developing storm in middle altitudes. The lower these temperatures are, the more intensive phenomena are to be expected. A similar rule can be set up on the base of the difference between *Tl* and *Tg*. With the decreasing value of that temperature difference we can expect more extreme events developing in the storm as shown in *Table 2*.

Finally, the temperature of the level where particles reach the radius of 14 μm is the precipitation threshold temperature. With the decreasing temperature of the level of 14 μm particle radii, stronger updraft is indicated inside the cloud. Indirectly, it may be deduced that a more severe storm will develop (see *Table 2*). Additionally, the knowledge of the cloud base temperature indirectly helps the improvement of the convection and precipitation (*Zhu et al.*, 2014) forecasts. It helps to reveal the top of boundary layer and the water vapor mixing ratio, which helps to calculate CAPE more accurately (*Zhu et al.*, 2014).

Table 2. Statistical values: mean, standard deviation, median, mode, 10% percentile, and 90% percentile for the following characteristics: *re* at the cloud base, *re* at the cloud top, *Tl, Tg,* and *T14µm,* the difference of *Tl* and *Tg* all split by weather events. Zeros mean that no appropriate value was found, a blank space was not calculated as explained in Section 5.1.

EVENT	STATISTICS	*re base* (µm)	*Tl* (°C)	*Tg* (°C)	*T14µm* (°C)	*Tl–Tg* (°C)
TOR	MEAN + SD	6.1 ± 0.9	–25.1 ± 6.1	–37.4 ± 5.8	–24.5 ± 6.8	12.3 ± 4.1
TOR	MEDIAN	6	–26.5	–38	–26.5	11.5
TOR	MODE	6	–28	–38	–28	10
TOR	10 % PERC.	5.4	–31.5	–43.8	–31.5	8.5
TOR	90 % PERC.	7	–18.5	–30	–15	18
GR	MEAN + SD	6.5 ± 1.3	–22.8 ± 6.7	–35.5 ± 4.1	–23.7 ± 4.7	12.7 ± 6.5
GR	MEDIAN	6	–25	–38	–25	12
GR	MODE	7	–25	–38	–27	8
GR	10 % PERC.	5	–30	–40	–28	6
GR	90 % PERC.	7	–12	–31	–17	23
+RA	MEAN + SD	7 ± 0	–20 ± 0	–33 ± 0	–22 ± 0	13 ± 0
+RA	MEDIAN	7	–20	–33	–22	13
+RA	MODE	0	0	0	0	0
+RA	10 % PERC.	7	–20	–33	–22	13
+RA	90 % PERC.	7	–20	–33	–22	13
FC	MEAN + SD	7.3 ± 0.5	–19.7 ± 5.6	–32.5 ± 2.5	–20.7 ± 4.2	14 ± 4
FC	MEDIAN	7	–22	–32.5	–22	14
FC	MODE	7	0	0	0	0
FC	10 % PERC.	7	–24.4	–34.5	–24.4	10.8
FC	90 % PERC.	7	–14	–30.5	–16.4	17.2
NONSEVERE	MEAN + SD	8.8 ± 0.8	–17.5 ± 4.6	–30.5 ± 0.5	–19.8 ± 5.2	11.5 ± 1.5
NONSEVERE	MEDIAN	8.5	–19	–30.5	–21	11.5
NONSEVERE	MODE	8	0	0	0	0
NONSEVERE	10 % PERC.	8	–21.4	–30.9	–24.7	10.3
NONSEVERE	90 % PERC.	9.7	–12.4	–30.1	–13.8	12.7

GR – hail; TOR – tornado; +RA – heavy rain; FC – funnel cloud

As can be expected, *Table 1* shows that no single value (as *Tl*, *Tg*, etc.) can provide any relevant and complete information about the severity of a developing storm. However, it can show values from which the storm can be predicted to become severe, but there is no strict boundary in values between individual severe event values in *Table 1*. This confirms that we need to analyze the *T-re* profile as a whole to see all connections above and under a specific value in the profile.

Better information about threshold values between individual severe events is provided with statistically processed data (mean values and standard deviations) in *Table 2*.

Table 2 also provides some basic statistical quantities that were applied to the values of *re base* (μm), *Tl* (°C), *Tg* (°C), *T14μm* (°C), and *Tl-Tg* (°C). The quantities are mean, standard deviation (SD), median, mode, 10% percentile, and 90% percentile for each severe weather event. They are presented in *Table 2*.

The analysis of the statistical quantities showed that there is a good transition value of *re base*, *Tl*, *Tg,* and *T14μm,* which would clearly distinguish severe and nonsevere situations. Moreover, these features may distinguish different severe accompanying phenomena in most cases. However, it is still faster and easier to analyze the gained *T-re* profiles as an image without any calculations. Some basic features of severe and nonsevere *T-re* profiles gained from *Tables 1* and *2* are mentioned in the Section 6.

Not every nonsevere situation is mentioned in *Tables 1* and *2*, because the values of tracked features are always typically nonsevere. Nonsevere situations, especially those with rain and without thunderstorms which could potentially form a new "non-thunderstorm" category were also analyzed, but the values of their tracked features cannot be included in the statistical analysis for the nonsevere category. These values were not in our focus. In addition, they would shift the gained statistical severe/nonsevere threshold results closer to the "non-thunderstorm" values, i.e., far from the desired threshold values. Furthermore, these values would enlarge the standard deviation of the tracked values in the nonsevere category, which would cause false alarm cases.

5.1. Nonsevere situations

Nonsevere situations, still significant in terms of convection, which were included in the statistics can be considered a threshold state between nonsevere and severe situations. There were thunderstorms without any severe accompanying phenomena observed. The definitely non-thunderstorm convective situations have only a small vertical extent with cloud tops typically below 6 km, and particles grow to larger sizes in the coalescence zone at lower levels rather than in the cases presented here. As the analysis reveals, in nonsevere (threshold) situations the coalescence zone to (*Tl*) does not usually reach the –20 °C level as it can be seen in *Table 2*. There are mostly large particles in the coalescence growth zone with a radius of about 15 μm. Near the level of –20 °C or lower (towards the ground), the particles start to enlarge their sizes quickly. The coalescence in nonsevere situations has a larger effect compared to the severe situation. Slower updrafts allow particles grow to larger sizes as they stay in a relatively thin area in contrast to severe situations. A radius of about 30 μm is usually reached near the temperature of about –30 °C. The particles freeze heterogeneously, and their sizes enlarge quickly in this zone. Cloud bases very often develop between temperatures of 10 °C and 0 °C, with the highest frequency between temperatures of 5 °C and 0 °C.

Nonsevere thunderstorms with large Cbs can reach a level of –40 °C. The analyzed profiles show a noticeable bent shape, and there is no linear part of the graph.

It is important to remember that the large extent of the updraft zone and low temperatures near cloud tops indicate hail or other severe attendant phenomena. Even if there were a strong updraft in clouds which did not reach very low temperatures, severe storms would not develop.

In the situation where only rain was observed, even the values mentioned above are not reached, and the profiles are shaped towards larger particles at lower temperatures (to the right side).

The following threshold values between nonsevere and severe storms were found: *re base* 8.8 ± 0.8 μm, *Tl* –17.5 ± 4.6 °C, *Tg* –30.5 ± 0.5 °C, and *T14μm* –19.8 ± 5.2 °C (*Table 2*). The high values of standard deviations are caused by the situation on July 20th, 2013, which is included in the statistics. This is a typical nonsevere situation with higher tracked temperatures, which causes the enlargement of the standard deviation. The situations with smaller *re base* and lower temperatures (*Tl, Tg, T14μm*) are prone to grow into storms with severe attendant phenomena. Estimating the difference of *Tl* and *Tg* for the nonsevere cases is absolutely irrelevant, because the glaciation phase with *Tg* value mostly did not develop.

5.2. Severe situations

T-re profiles of severe situations (convective storms with dangerous attendant phenomena) reach much higher levels than in the case of nonsevere situations. The profiles are steeper in the thicker zone, mostly in their lower part, with this zone being frequently linear or nearly linear as the updraft pushes the particles higher with a high speed. A radius of 14 μm is mostly reached by the level of –20 °C or above, when the clouds include ice particles. The particles do not grow fast because they do not stay in the coalescence zone for a long time. When the ice particles are small at a level of around –40 °C, it indicates vigorously growing cells with a strong updraft inside. Cloud droplets freeze homogenously there, and the radius is usually less than 35 μm in this zone. Cloud particles with radii less than 14 μm often fill the zone of the temperature difference of 30 °C or more.

In the case of 2–3 cm hail occurrence, a particle radius of 9 μm was observed up to the level of –22 °C. In the case of 3 cm hail and 20 mm/h rain, a radius of 14 μm was identified at a level of about –28 °C. With larger hail (4 cm), the radius of 14 μm reached a level of about –30 °C.

Table 2 shows the mean values and standard deviations of tracked features for different severe storms with various attendant phenomena. It clearly shows that the *re base* decreases with increasing the severity of the accompanying phenomena of a storm, and the same is valid for the mentioned temperatures *Tl*, *Tg*, and *T14μm.*

The illustrative interpretation is depicted in boxplots, in *Figs. 3a-d*.

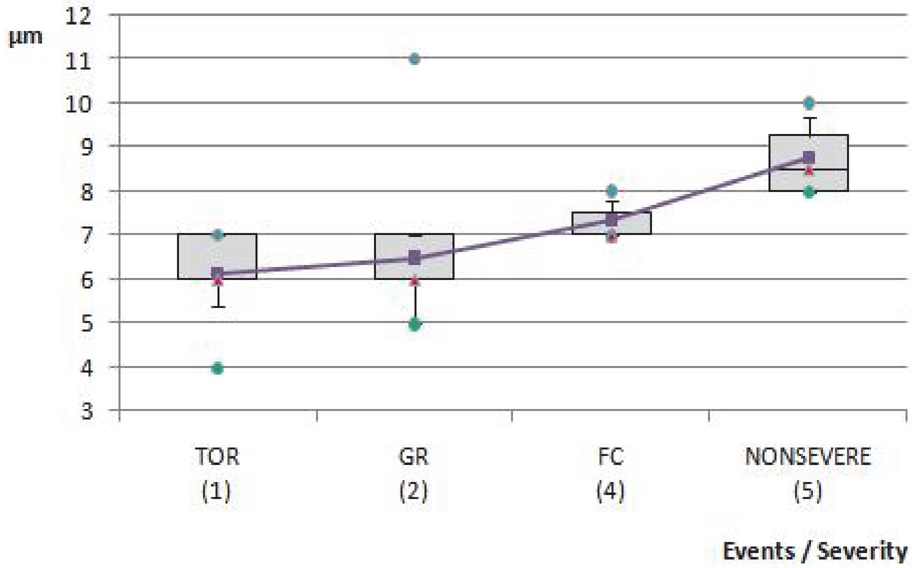

Fig. 3a. Boxplots of *re base* (µm) for different attendant phenomena of storms. Decrease of *re base* with an increase in the attendant phenomena severity represented by the different group of attendant phenomena. Number 1 was assigned to the most intensive case (tornado) decreasing to number 5 (nonsevere) as explained in Section 5. The case of heavy rain (3) is not included because only one case was recorded. The bottom of the box of *re base* represents the value of the 1st quartile, the middle dark line in the box with the red triangle is the median, the violet rectangle inside each box is the mean, and the top of each box is the 3st quartile value. The bottom and top of each whisker are the 10% and 90% percentiles, and the green and blue dots are the maximum and minimum, respectively. In the values of the mean for tracked features depicted by the box profiles, a clear decrease in tracked size with increasing severity of storms can be seen.

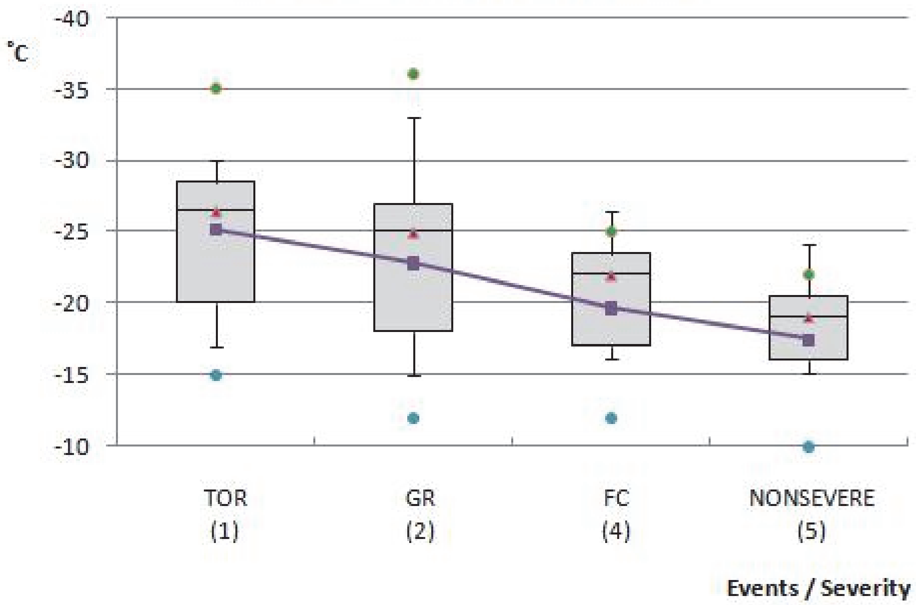

Fig. 3b. The same as *Fig. 3a* but for *Tl* (°C) for different attendant phenomena of storms.

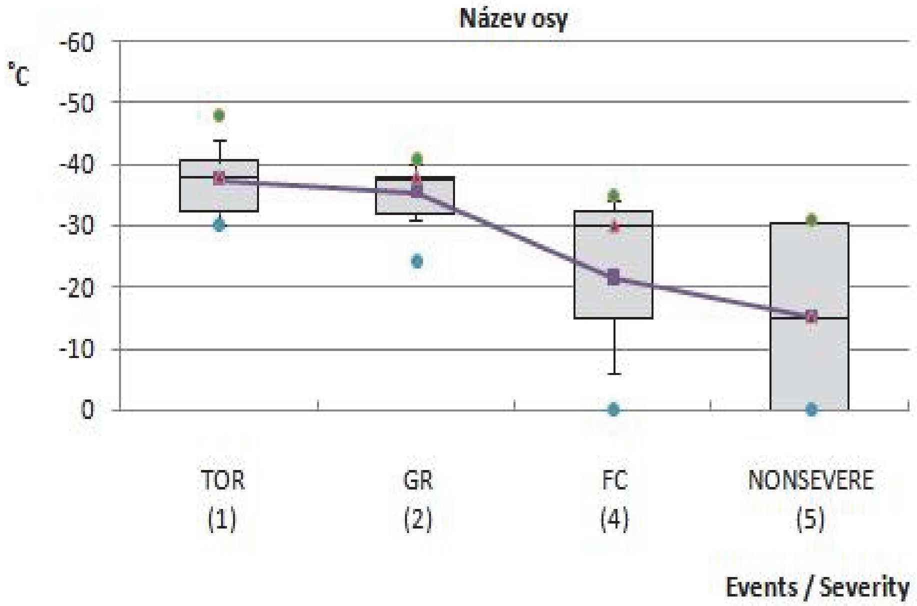

Fig. 3c. The same as *Fig. 3a* but for *Tg* (°C) for different attendant phenomena of storms.

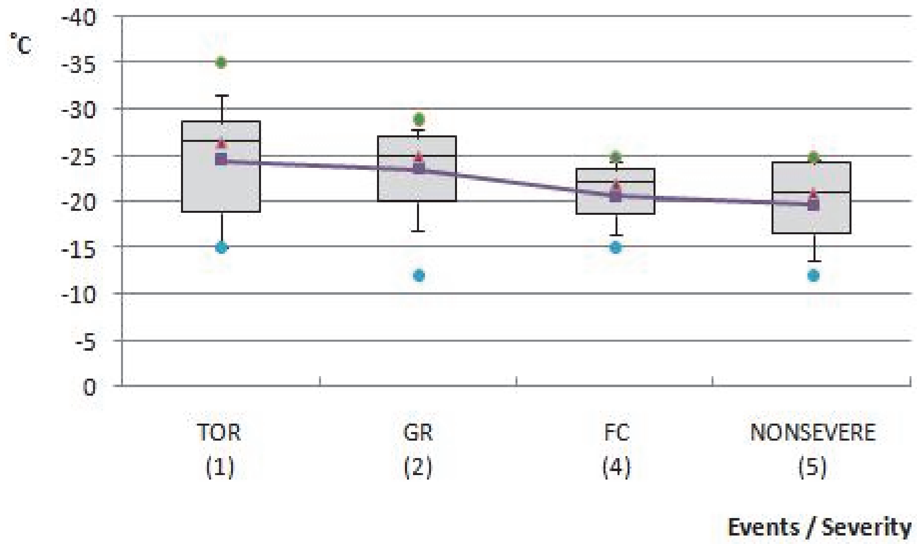

Fig. 3d. The same as *Fig. 3a* but for *T14μm* (°C) for different attendant phenomena of storms

The difference of *Tl* and *Tg* as presented in *Table 2* decreases with an increase in storm severity. In cases with funnel cloud occurrence, the difference was 14 ± 4 °C, in heavy rain cases 13 ± 0 °C, in hail cases 12.7 ± 6.5 °C, and in tornadic cases 12.3 ± 4.1 °C.

Furthermore, correlation analysis was performed. It represents a statistical method which describes the relationship between two variables. The first step was the compilation of the correlation matrix (*Table 3*), which includes the correlation coefficients of all the couples of variables, here the tracked features of *T-re* profiles (*re base*, *Tl*, *Tg*, *T14μm*). In this case, correlation represents the mutual relationship between two tracked features. The level of correlation is influenced by the value of the correlation coefficient R that attains values from –1 to +1. There is no relationship between the studied variables if the value of R equals 0. A positive value close to +1 represents direct proportion (a positive correlation), –1 on the other hand represents indirect proportion (a negative correlation). Taking into account our results where all the values of R were higher than 0.92 (*Fig. 4*), a significant positive linear correlation for tracked features was found.

Table 3. Correlation coefficients (R) of all couples of tracked features (*re base, Tl, Tg, T14µm*). The values of correlation coefficient represent significant linear correlation of all tracked features, because all the values are close to 1.

	***re* base (µm)**	**Tl (°C)**	***Tg* (°C)**	***T14µm* (°C)**
***re* base (µm)**	1.00			
***Tl* (°C)**	0.92	1.00		
***Tg* (°C)**	0.93	1.00	1.00	
***T14µm* (°C)**	0.92	0.97	0.98	1.00

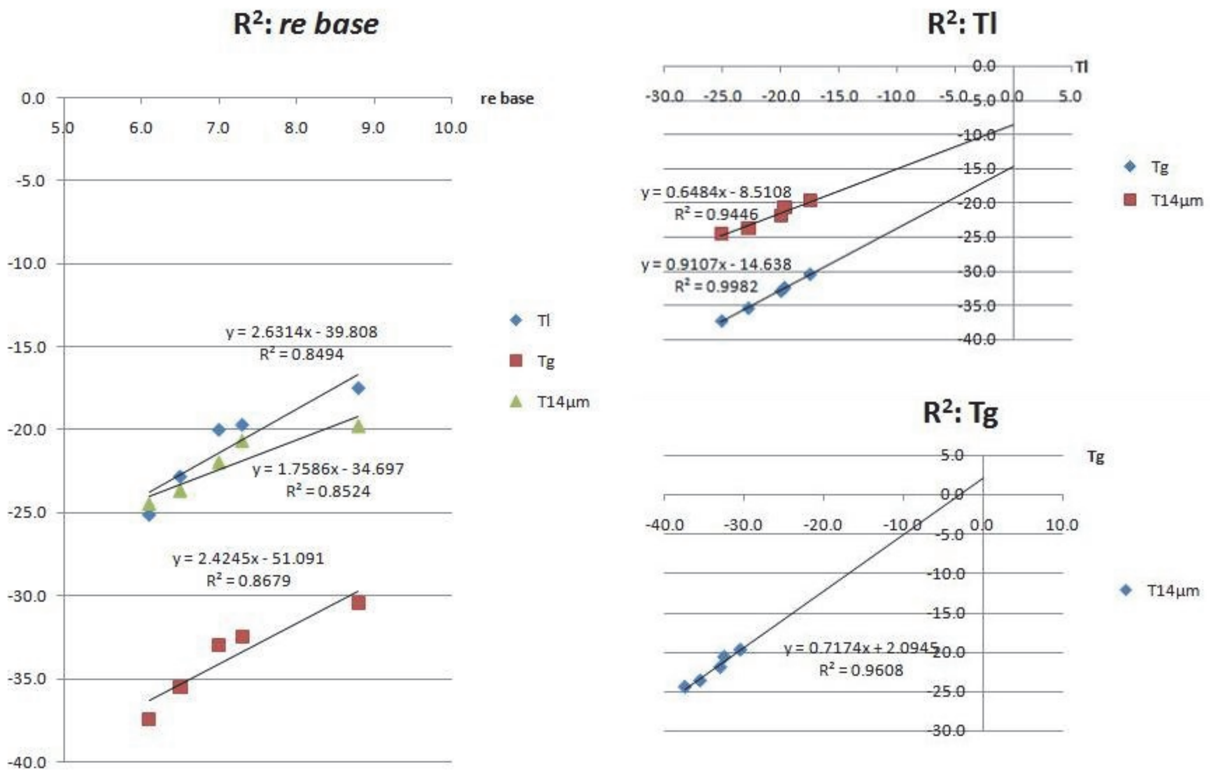

Fig. 4. Coefficient of determination (R^2) of *re base* and other tracked features of *T-re* profiles (*Tl*, *Tg*, *T14µm*).

The correlation matrix (Table 3) provides the correlation coefficients (R) for all couples of tracked features (*re base*, *Tl*, *Tg*, *T14µm*). All couples are in significant linear correlation, since R is higher than 0.92 for all. The determination coefficients confirm that the line equation confidence level is higher than 84%. Linear coefficients are statistically significant at the significance level 0.05.

Fig. 4 shows the linear correlation of all couples of tracked features where the horizontal axis represents one feature and the vertical axis represents the other feature for each couple. Their correlation is provided by the equation of the line and R^2 represents the suitability of the model.

The knowledge of linear correlation for tracked features of *T-re* profiles allows us to find a model of correlation for those features. On the basis of the results, the model can only provide a simple mathematical forecast, but it cannot result in certainty. That trend predicts next evolution of features according to the previous evolution. Every mathematical forecast has its own confidence level, which represents the reliability of that forecast. The confidence level (*Table 4*) is expressed by the determination coefficient (R^2) that attains values from 0 to 1, where 1 means 100% confidence. The determination coefficient (R^2) of our data was always equal to more than 0.84; thus, the confidence level of the model of the regression function is always higher than 84%.

Table 4. Determination coefficient (R2) of all couples of tracked features (*re base, Tl, Tg, T14µm)*

	re base **(µm)**	***Tl*** **(°C)**	***Tg*** **(°C)**
Tl **(°C)**	0.8494		
Tg **(°C)**	0.8679	0.9982	
T14µm **(°C)**	0.8524	0.9446	0.9608

The revealed linear correlation of *re base*, *Tl*, *Tg,* and *T14µm* made it clear that the mentioned temperature *T14µm* decreases with the increasing severity of the attendant phenomena of storms and a proportional decrease of *Tl* and *Tg* as well as *re base* with the increasing severity of the attendant phenomena of storms. This correlation analysis confirms previously specified rules of *T-re* profiles in severe weather analysis and forecasting (*Rosenfeld et al.*, 2008). With the increasing severity of weather events, the *T-re* profiles actually shift to the left side of the graph (to smaller *re*) and extend higher (to lower temperatures) (see *Fig. 1* and *Fig. 2* to compare).

The determination coefficients for all couples of tracked features were calculated (*Table 4*). The value expresses in percent the reliability of the line equation of two features. All the values exceed a value of 84%, thus the equation describes the correlation between two features better than 84%.

The processed data are graphically presented in *Fig. 4*, which proves the correlation of individual tracked features, their trend functions and confidence level. Similarly, the trend functions for *Figs. 5a-d* were obtained. The graphs reveal the correlation of individual tracked features and the severity of attendant phenomena of a storm, trend function, and determination coefficient (R^2), where the confidence level of each model is greater than 90%.

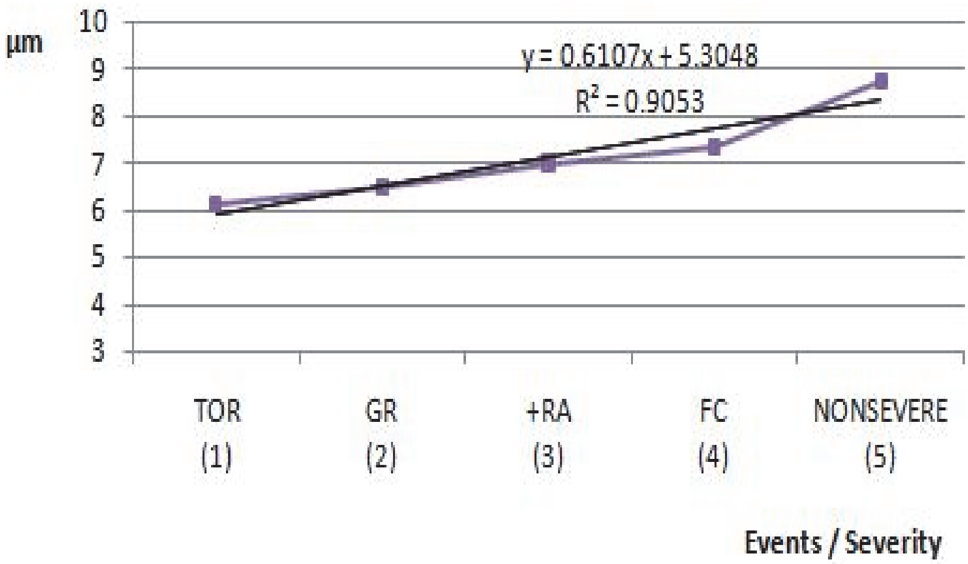

Fig. 5a. Coefficient of determination of *re base* for different groups of attendant phenomena of storms.

Consider *re base* as a mean of *re base*. Gaining high value of R (correlation coefficient) expresses the linear correlation of *re base* and the intensity of storms represented by the different group of attendant phenomena. The equation of the line (see the graph) describes the data at the significance level of 90% what is represented by the value of the coefficient of determination (R^2) to be 0.9053.
According to the values gained from the graph and the equation of the line we can find the storm severity. If, for example, the *re base* equals six, then the equation gives the stage of a tornado, but this can also indicate other storm stages (TOR, GR, etc.). The only result is that the storm stage could be a tornado. All other tracked features (*Tl*, *Tg* or *T14μm*) have to be evaluated as well.

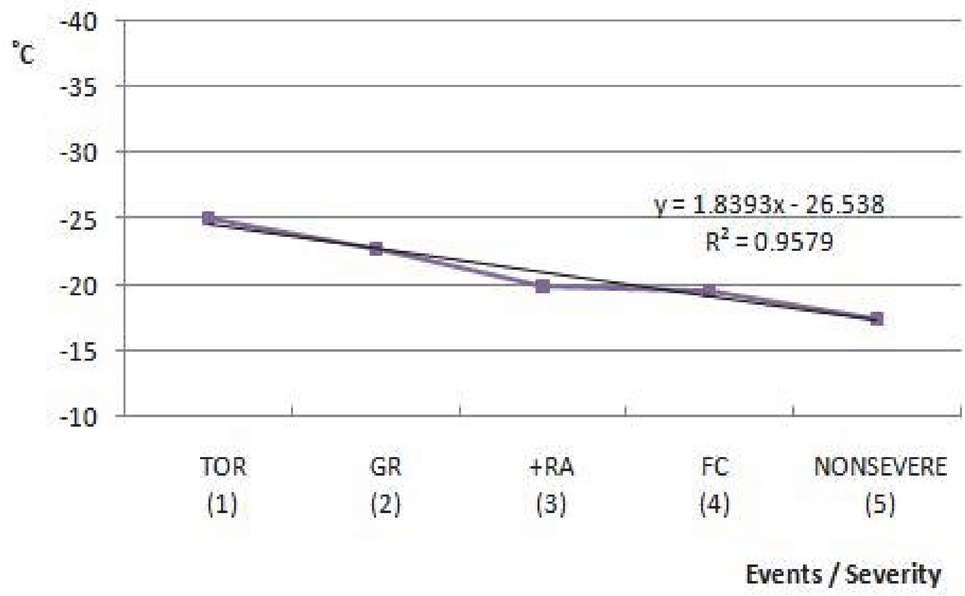

Fig. 5b. The same as *Fig. 5a* but for *Tl* for different groups of attendant phenomena of storms.

Consider *Tl* as a mean of *Tl*. A high value of R (correlation coefficient) expresses the linear correlation of *re base* and the intensity of storms represented by the different group of attendant phenomena. Significant linear correlation was found at the level of 95.8%.

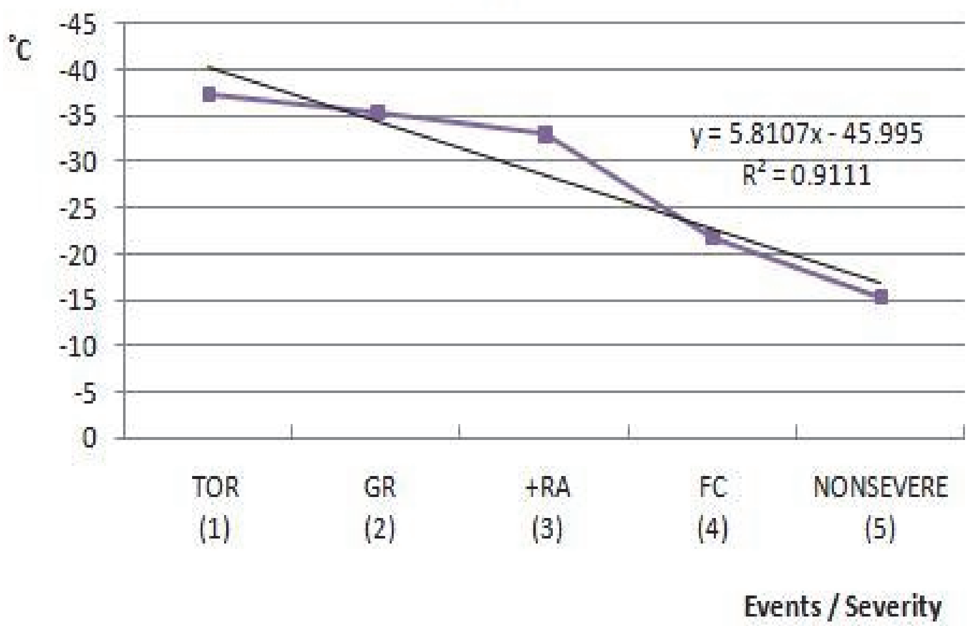

Fig. 5c. The same as *Fig. 5a* but for *Tg* for different groups of attendant phenomena of storms

Consider *Tg* as a mean of *Tg*. Gaining a high value of R (correlation coefficient) expresses the linear correlation of *re base* and the intensity of storms represented by the different group of attendant phenomena. Significant linear correlation was found at the level of 91.1%.

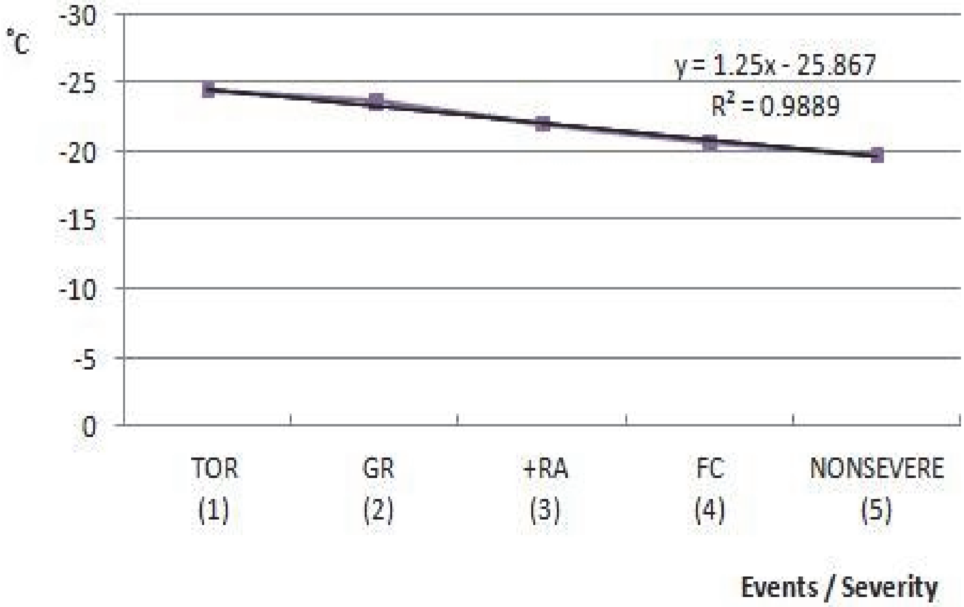

Fig. 5d. The same as *Fig. 5a* but for *T14μm* and the intensity of attendant phenomena of storms.

Consider *T14μm* as a mean of *T14μm*. Gaining a high value of R (correlation coefficient) expresses the linear correlation of *re base* and the intensity of storms represented by the different group of attendant phenomena. Significant linear correlation was found at the level of 98.9%.

Individual graphs and models of functions, regardless of the R^2 value, cannot be considered as decisive. In addition, it was proved that one single tracked feature cannot be used as a unique storm severity forecast element. All the tracked features, the shape of the *T-re* profile and its position and extent should be studied. As it is demanding to gain all the tracked features, to find all their correlations, and to find which variables support the model, it is also very difficult to assemble a global model of the tracked features for making storm severity decisions. It would probably also request more storm cases observation, which requires the gathering of automated data.

The linear correlation of *re base* and the tracked temperatures allows us to simplify the description of the *T-re* profiles. In an ideal case, it is possible to divide the individual part of a profile to individual lines defined by the temperatures *Tl* and *Tg* (*Fig. 1a-f*). As a matter of fact, the profile is a non-ramp fiction due to the vertical axis inversion, which corresponds to the real temperature decrease in the atmosphere. As has already been mentioned, one of the severe storm signs is the long linear (or nearly-linear) lower part of a *T-re* profile, rising to the breaking point of *Tl*.

This analysis should be considered a demonstration in which the independent dataset was used to test the previously derived relationships (*Rosenfeld et al*., 2008) requested by *Rosenfeld et al*. (2008). It has confirmed the value of the methodology for nowcasting of severe weather events.

Fig. 6 presents graphically the number of events reported (blue) and forecasted (red) in a given hour. Nearly 30% of the reported cases occurred at 12–14 UTC and nearly a similar percentage at 16–18 UTC. The prediction of a severe event was mostly (45%) performed at 12–14 UTC, which is in good agreement with severe weather occurrence, subsequently at 10–12 UTC.

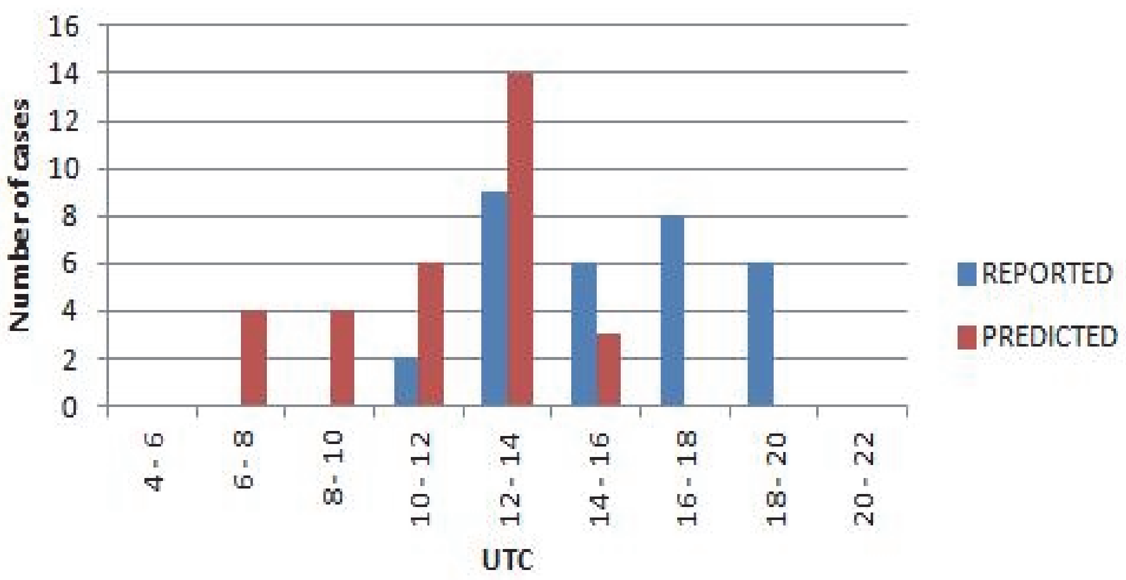

Fig. 6. Time distribution of reported (blue) and predicted (red) severe attendant phenomena of storms.

The forecasting skill of the *T-re* method was statistically evaluated (*Fig. 7*) comparing the time of the reported event (i.e., not the time of the first occurrence of the event) of the European Severe Weather Database and the time of our own severe event forecast. We compared the time of forecast and the time of the report of the event intentionally, because it is very complicated to estimate the time of first occurrence of the event without any appropriate confirmed observation. *Fig. 7* graphically shows the most frequent time difference of the forecast of an event before it was reported as discussed above. 68 percent of the predictions of severe weather were performed about two hours before its report, which is a good advantage for preventive measures. *Jurkovic et al.* (2015) found the ability of a *T-re* profile to reveal severe updrafts inside clouds 10-20 minutes in advance before hail start to fall out of the clouds. For example, the formation of hailstone with a size of 1 cm does not usually last longer than 1 hour.

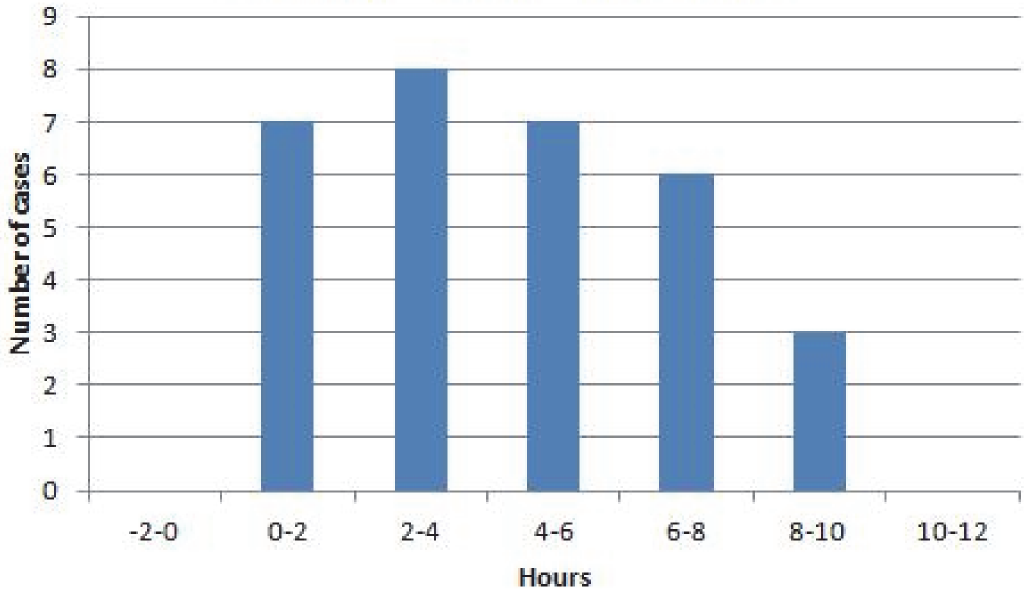

Fig. 7. Numbers of severe weather events according to the time difference of predicted and reported events (i.e., not the time of the first occurrence) as discussed in Section 5.2. Large intervals can be the consequence of inaccuracy of the detection of the precipitation type and amount on the ground.

Jurkovic et al. (2015) confirmed also that deep convective clouds which are associated with greater updraft speed are filled by smaller particles with a *re* of 15–20 μm above the level of –30 °C and a *re* of 30 μm above the level of –40 °C. He also stated the basic shapes of *T-re* profiles and other features of severe storm clouds in Europe (*Jurkovic et al*., 2015). Nonsevere storms on the other hand reveal a very different dependence of particle size on temperature. Large particles (*re* more than 35 μm) are frequently found below the level of –20 °C (*Jurkovic et al*., 2015).

There were no failed predictions of severe storms occurrence arising from the background of the method. According to cloud microphysics rules which can be depicted in gained profiles, failed predictions of severe storms cannot occur. Some people may incorrectly forecast different severe cases from others.

6. Discussion

It is apparently not possible to determine the absolute exact threshold values of *T* and *re* between different severe phenomena. It is important to analyze the thickness of the zone with small particles (less than 15 μm), the whole vertical extent of cloud cells and the shape of profiles in all their parts as well as the auxiliary values, such as *Tl*, *Tg* and *T14μm* etc. The mean values of *Tl* and *T14μm* followed by the mean values of *re base* and *Tg* presented in *Table 2* for each severe event could, on the other hand, are considered being a hint in distinguishing of different severe attendant phenomena of developing storms. These satellite-based predictors are considered to be at least as good as, for example, frequently used atmospheric sounding predictors and are much more detailed in time and space (*Rosenfeld et al.*, 2008). They are able to vary in time, because they are recalculated with every new satellite observation, which allows them to react to actual cloud development. When applied to multispectral geostationary satellite data, the *T-re* method provides us with a typical storm signature before these clouds are revealed by weather radar. Therefore, additional time to detect a severe storm is provided, although with lesser spatial accuracy compared to weather radars (*Rosenfeld et al.*, 2008). In general, it can be concluded that the profiles in Central Europe start at lower temperatures compared to those from the US (approximately about 5–10 °C), and the values *Tg* and *Tl* are observed at higher levels as well. The crucial point is that the cloud particle diameters are usually about 3–5 μm larger near the cloud base and again at higher levels compared to those from the US. The differences can be due to different instruments and resolution, not necessarily caused only due to physical features of air mass.

In some cases, the profiles indicate strong updrafts even during forenoon, but the dangerous events are reported in the evening.

For all presented severe situations, the mean particle effective radius at the cloud base is found to be between 6.0 and 7.3 μm as presented in *Table 2*. Tornadic situations, considered the most severe event, reveal the second highest mean of particle effective radius at the cloud base, but the smallest median together with hail and heavy rain cases. Small radii, about 6 μm or even smaller at the cloud base indicate a higher probability of tornado occurrence. There are also clear indications that smaller *Tl* and *T14μm* indicate greater severity of an event, the same for *Tg* can be said in most cases as well. All the severe situations presented in *Table 1* show smaller *Tg* and *Tl* difference in mean values (≤ 2 °C) than nonsevere situations (10 °C). Some specific connections similar to our findings were stated by *Sporre et al.* (2014). They clearly mentioned that clouds with greater vertical extent have higher precipitation rates compared to less developed clouds. His study also confirms that meteorological parameters such as atmospheric instability or cloud vertical extent affect the precipitation amount measured on the ground more than aerosols.

Presenting some statistically processed values provides threshold values as well as other described rules of specified temperatures and their relationships, but in some cases it does not describe the situation of *T-re* profiles the best way. Statistical values sometimes do not strictly differentiate between particular severe events, because analyzed values (such as *Tg* or *Tl*) are generalized too much. Thus, it is crucial to analyze the *T-re* profiles as a unique situation description, just because every thunderstorm is unique with different *T-re* values and also not every tornado is the same. Human forecasters are much more successful at severe weather forecasting compared to existing automated systems (*Doswel*, 2014), and with help of other analysis tool they could be even better.

The method of severe storm intensity forecasting with the help of *T-re* profiles applied to the MSG satellite data in the region of Central Europe seems to be apparently successful.

7. Conclusions

The basic principle of the presented theory is the analysis of cloud particle profiles based on satellite observation in different spectral channels to help forecast and identify a potentially dangerous storm. It is possible to generate *T-re* profiles that represent the microphysical composition of clouds with special software. The analysis of archived satellite data selected according to dangerous weather reports as well as real-time data from the MSG reception station was carried out, and the applicability of these profiles were evaluated in Central Europe for the first time. The nonsevere threshold situations were analyzed in order to confirm the potential of this tool also for these non-threatening cases. *T-re* profiles have proved to be a useful tool for nowcasting during severe convective storm situations in this region. However, different air mass types play a crucial role in the thermodynamic condition above different areas. The profiles from Central Europe revealed, for example, the shift in the temperature and size of cloud particles compared to profiles from other continents, as mentioned in Section 4. Also *Tl* and *Tg* values were usually higher, which represents lower temperatures than in the profiles of *Rosenfeld et al*. (2008).

The *T-re* method can help to reveal the areas apt to produce severe weather phenomena mostly one or two hours in advance, sometimes even sooner, analyzing cloudy areas from morning hours in days with expected intense convection. It is a very simple software to use and quickly provides a microphysical preview of clouds. This research revealed the fact that it is crucial to see the whole profile with all of its features to be able to create a forecast of severity for a developing storm. A stand-alone value such as *Tl* or *Tg* without knowing any other features of a *T-re* profile cannot provide complete and exhaustive relevant information to use in forecasting. It can however provide an initial impulse in distinguishing between severe and nonsevere cases, and in most cases, in distinguishing between particular severe cases. After familiarization with a typical *T-re* profile for severe situations, a local forecaster should be able to use it successfully to improve the severe weather nowcasting processes. With the help of this nowcasting tool, specific and more accurate weather warnings for particular areas can be issued to protect property or even lives.

Acknowledgements: This project was supported by the Specific Research Fund of the Faculty of Mathematics and Physics, Charles University, Prague, number SVV-2011-263308. A special thanks goes to *Dr. Itamar Lensky*, Bar-Ilan University, Israel, the provider of the MSG_RGB software and EUMETSAT for providing the satellite data.

References

Brázdil, R., Chromá, K., Dobrovolný, P., and *Černoch*, Z., 2012: The Tornado History of the Czech Lands, AD 1119-2010. *Atmos. Res. 118*, 192–204.

Brooks, H.E., 2012: Severe Thunderstorm and Climate Change. *Atmos. Res. 123*, 129–138.

Doswel, C.A.III, 2014: Severe Convective Storms in the European Social Context. *Atmos. Res. 158-159*, 210–215.

Dotzek, N., 2003: An updated estimate of tornado occurrence in Europe. *Atmos. Res. 67-68*, 153–161.

Dotzek, N., Groenemeijer, P., Feuerstein, B., Holzer, A.M., 2009: Overview of ESSL's severe convective storms research using the European Severe Weather Database ESWD. *Atmos. Res. 93*, 575–586.

Field, C.B., Barros, V., Stocker, T.F., Qin, D., Dokken, D.J., Elbi, K.L., Mastrandrea, M.D., Mach, K.J., Platner, G.K., Allen, S.K., Tignor, M., and *Midgley, P.M.*, 2012: Managing the Risks of Extreme Events and Disaster to Advance Climate Change Adaptation. A Special Report of Working Groups I and II of the Intergovernmental Panel on Climate Change. Cambridge University Press, Cambridge, UK, New York, NY, USA, 582 pp.

Holzer, A.M., 2001: Tornadoes Climatology of Austria. *Atmos. Res.* 56, 203–211

Horváth, Á. and *Geresdi, I.*, 2003: Severe Storms and Nowcasting in the Carpathian Basin. *Atmos. Res. 67-68*, 319–332

Jurković, P.M., Mahović, N.S., and *Počakal, D.*, 2015: Lightning, Overshooting Top and Hail Characteristics for Strong Convective Storms in Central Europe. *Atmos. Res. 161-162*, 153-168.

Lensky, I., 2009: User Guide for MSG_RGB. Personal communication.

Lensky, I. and *Rosenfeld, D.*, 2005: The Time-Space Exchangeability of Satellite Retrieved Relations Between Cloud Top Temperature and Particle Effective Radius. *Atmos. Chem. Phys.6*, 2887–2894.

Lensky, I., Shiff, S., 2007: Using MSG to monitor the evolution of severe convective storms over East Mediterranean Sea and Israel and its response to aerosol loading. *Adv. Geosci. 12*, 95–100.

Martins, J.V., Marshak, A., Remer, L.A., Rosenfeld, D., Kaufman, Y.J., Fernandez-Borda,R., Koren, I., Yubko, V., and *Artaxo, P.*, 2007: Remote Sensing The Vertical Profile of Cloud Droplet Effective Radius, Thermodynamic Phase and Temperature. Atmos. Chem. Phys. Discuss. 7, 4481–4519.

Melani, S., Cattani, E., Levizzani, V., Cervino, M., and *Torricella, F.*, 2003: Radiative effects of simulated cirrus clouds on top of a deep convective storm in MSG SEVIRI channels. *Meteorol. Atmos. Phys. 83*, 109–122.

Pfeifer, M., Yen, W. ,Baldauf, M., Craig, G., Crewell, S., Fischer, J., Hagen, M., Huhnerbein, A., Mech, M., Reinhardt, T., Schroder, M., and *Seifert, A.*, 2010: Validating Precipitation Forecast Using Remote Sensor Synergy: A Case Study Approach. Meteorol. Zeit. 19, 601–6017.

Roberts, R.D. and *Rutlege, S.*, 2003: Nowcasting Storm Initiation and Growth Using GOES-8and WSR-88D Data. *Weather Forecast. 18*, 562–584.

Rosenfeld, D., Fischman, B., Zheng, Y., Goren, T., and *Giguzin, D.*, 2014: Combined Satellite and Radar Retrievals of Drop Concentration and CCN at Convective Cloud Base. *Geophys. Res. Let. 41*, 3259–3265.

Rosenfeld, D. and *Lensky, I.*, 1998: Satellite-Based Insights into Precipitation Formation Processes in Continental and Maritime Convective Clouds. *Bull. Amer. Meteorol. Soc. 79*, 2457–2476.
Rosenfeld, D., Woodley, W.L., Krauss, T.W., and *Makitov, V.*, 2006: Aircraft Microphysical Documentation from Cloud Base to Anvils of Hailstorm Feeder Clouds in Argentina. *J. App. Meteorol. Clim. 45*, 1261–1281.
Rosenfeld, D., Liu, G., Yu, X., Zhu, Z., Dai, J., Xu, X., and *Yue, Y.*, 2013: High Resolution (375m) Cloud Microstructure as Seen from The Satellite NPP/VIIRS Satellite Imager. *Atmos. Chem. Phys. Discus. 13*, 29845–29894.
Rosenfeld, D., Woodley, W.L., Lerner, A., Kelman, G., and *Lindsey, D.T.*, 2008: Satellite Detection of Severe Convective Storms by Their Retrieved Vertical Profiles of Cloud Particle Effective Radius and Thermodynamic Phase. *J. Geophys. Res.113*, D04208.
Setvák, M., 1989: Convective Storms - The AVHRR Channel 3 Cloud Top Reflectivity as A Consequence of Internal Processes. Proc. 5th WMO Conference of Weather Modification and Applied Cloud Physics, Beijing, China, WMO/TD 269, 109-112.
Shiqiang, F. and *Zhemin, T.*, 2001: On the helicity dynamics of severe convective storms. *Adv. Atm. Sc. 18*, 67–86.
Sporre, M. K., Swietlicki, E., Glantz, P., and *Kulmala, M.*, 2014: A long-term satellite study of aerosol effects on convective clouds in Nordic background air. Atmos. *Chem. Phys. 14*, 2203–2217.
Tokay, A. and *Short, D.A.*, 1996: Evidence from Tropical Raindrop Spectra of the Origin of Rain from Stratiform versus Convective Clouds. *J. Appl. Meteorol. 35*, 355–371.
Tolasz, R., Brázdil, R., Bulíř, O., Dobrovolný, P., Hájková, L., Halásová, O., Hostýnek, J., Janouch, M., Kohout, M., Krška, K., Křivancová, S., Květoň, V., Lepka, Z., Lipina, P., Macková, J., Metelka, L., Míková, T., Mrkvica, Z., Možný, M., Nekovář, J., Němec, L., Pokorný, J., Reitschläger, J.D., Richterová, D., Rožnovský, J., Řepka, M., Semerádová, D., Sosna, V., Stříž, M., Šercl, P., Škáchová, H., Štěpánek, P., Štěpánková, P., Trnka, M., Valeriánová, A., Valter, J., Vaníček, K., Vavruška, F., Voženílek, V., Vráblík, T., Vysoudil, M., Zahradníček, J., Zusková, I., Žák, M., and *Žalud, Z.*, 2007: Atlas podnebí Česka - Climate Atlas of Czechia. Český hydrometeorologický ústav, Praha, Univerzita Palackého v Olomouci, Olomouc.
Zheng, Y. and *Rosenfeld, D.*, 2015: Linear Relation between Convective Cloud Base Height and Updrafts and Application to Satellite Retrievals. *Geophys. Res. Let. 42*, 6485–6491.
Zheng, Y. and *Rosenfeld, D., Li, Z.*, 2015: Satellite Inference of Thermal and Cloud-Base Updraft Speeds Based on Retrieved Surface and Cloud-Base Temperatures. *J. Atmos. Sci. 72*, 2411–2428.
Zhu, Y., Rosenfeld, D., Yu, X., and *Li, Z.*, 2015: Separating Aerosol Microphysical Effects and Satellite Measurement Artifacts of the Relationship between Warm Rain Onset Height and Aerosol Optical Depth. *J. Geophys. Res. 120*, 7726–7736.
Zhu, Y., Rosenfeld, D., Yu, X., Liu, G., Dai, J., Xu, X., 2014: Satellite Retrieval of Convective Cloud Base Temperature Based on The NPP/VIIRS Imager. *Geophys. Res. Let. 41*, 1308–1313.
Zipori, A., Rosenfeld, D., Tirosh, O., Teutsch, N., and *Erel, Y.*, 2015: Effects of aerosol sources and chemical compositions on cloud drop sizes and glaciation temperatures. *J. Geophys. Res. 120*, 9653–9669.

Web references

Nowcastimg Thunderstorm Intensity from Satellite: A Review, *Robert M. Rabin*: http://www.ssec.wisc.edu/~rabin/paper/eumetsat/paper2_eumetsat.doc, 2015.
European Severe Weather Database: http://www.eswd.eu/, 2015.
European Severe Weather Database – Definitions: http://www.eswd.eu/cgi-bin/eswd.cgi?action =showdefinitions&lang=en_0, 2015.

Abbreviation list

CAPE – convective available potential energy
CCN – cloud condensation nuclei
CIN – convective inhibition
dBZ – radar reflectivity scale
EPS – EUMETSAT Polar System
ESSL – European Severe Storms Laboratory
ESWD – European Severe Weather Database
GOES – Geostationary Operational Environmental Satellites
MSG – Meteosat Second Generation
NOAA – National Oceanic and Atmospheric Administration
NWP – numerical weather prediction
Re – cloud particle effective radius
re base – cloud particle radius range near the cloud base
re top – cloud particle radius range near the cloud top
RGB – colored combination of satellite channels
RUC – rapid update cycle
SAFNWC– Satellite Application Facility on support to Nowcasting
T14μm – temperature of the level when particles reach a radius of 14 μm
Tg – temperature of the glaciation phase bottom
Tl – temperature of the top of the lower linear part of the profile
T-re – *T* represents cloud top temperature, *re* means particles effective radius
USA – The United States of America
WV – water vapor